

## Dysregulated cancer cell transdifferentiation into erythrocytes is an additional metabolic stress in hepatocellular carcinoma

Tumor Biology  
November 2018: 1–17  
© The Author(s) 2018  
Article reuse guidelines:  
[sagepub.com/journals-permissions](http://sagepub.com/journals-permissions)  
DOI: 10.1177/1010428318811467  
[journals.sagepub.com/home/tub](http://journals.sagepub.com/home/tub)



Abigail Hughes and Gurtej K Dhoot 

### Abstract

A number of human and canine hepatocellular carcinoma tissues showed clear signs of hypoxia indicated by HIF1 $\alpha$ -activation and the presence of large clusters of cells resembling erythrocytes at different stages of nuclear elimination without any defined endothelial cell lining or blood vessel walls. Differentiated erythrocytic identity of such cells in hepatocellular carcinoma tissues was apparent from their non-nucleated and evolving basophilic to eosinophilic staining characteristics. In addition to the fully differentiated non-nucleated mesenchymal cell clusters, the onset of erythroblastic transdifferentiation was apparent from the activation of Glycophorin A, a marker of erythrocytic progenitors, in some epithelial cancer cells. Activation of canonical Wnt signalling in such tumours was apparent from the expression of Wnt2 ligand and active  $\beta$ -catenin translocation into the nucleus indicating Wnt signalling to be one of the key signalling pathways participating in such cell transdifferentiation. Sonic hedgehog and bone morphogenetic protein signalling along with Sulfi/Sulf2 activation was also observed in such hepatocellular carcinoma tissue samples. The presence of stem cell markers and the cell signalling pathways associated with erythropoiesis, and the detection of messenger RNAs for both  $\alpha$  and  $\beta$  haemoglobins, support the assumption that hepatocellular carcinoma cells have the potential to undergo cell fate change despite this process being dysregulated as indicated by the lack of simultaneous generation of endothelial cell lining. Lack of blood vessel walls or endothelial cell lining around erythrocytic clusters was confirmed by non-detection of multiple blood vessel markers such as vWF, CD146 and smooth muscle  $\alpha$ -actin that were clearly apparent in normal and unaffected adjacent regions of hepatocellular carcinoma livers. In addition to the activation of Glycophorin A, transdifferentiation of some hepatocellular carcinoma hepatocytes into other cell fates was further confirmed by the activation of some stem cell markers, for example, NANOG and OCT4 transcription factors, not only by reverse transcription polymerase chain reaction but also by their restricted expression in such cells at protein level.

### Keywords

Cell signalling, hepatocellular carcinoma, cancer stem cells, transdifferentiation, erythroblasts/erythrocytes, Sulfi/Sulf2

Date received: 15 February 2018; accepted: 15 October 2018

### Introduction

Hepatocellular carcinoma (HCC), a leading cause of death worldwide,<sup>1,2</sup> is characterised by abnormal cell proliferation requiring adequate supply of oxygen and nutrients delivered through the blood supply, placing an unsustainable burden on patient metabolism.<sup>3</sup> Many tumours also exhibit a considerable proportion of necrotic tissue due to dysregulated cell signalling. This drives unsustainable cell fate or differentiation

options placing an additional metabolic burden on patient resources. Increasing evidence indicates that

---

Department of Comparative Biomedical Sciences, The Royal Veterinary College, London, UK

#### Corresponding author:

Gurtej K Dhoot, Department of Comparative Biomedical Sciences, The Royal Veterinary College, Royal College Street, London NW1 0TU, UK.  
Email: [tdhoot@rvc.ac.uk](mailto:tdhoot@rvc.ac.uk)



loss of regulation in cancer cell proliferation leads to excessive bioenergetic and biosynthetic requirements.<sup>4-8</sup> Therefore, it is not surprising that more than half of cancer patients suffer from cachexia, and nearly 30% of cancer deaths are a result of anaemia/cachexia rather than a direct result of tumour growth. Growing tumours face major metabolic challenges when nutrient and oxygen requirements outpace the limited supply via the normal vascular network. This could trigger the stimulation of angiogenesis and/or haemopoiesis to meet the metabolic demands of increased tumour growth. The generation of angiogenic and haemopoietic progenitors in an ordered fashion is a highly regulated growth process in the early embryo and during the revascularisation of the normal injured regenerating tissues.<sup>9</sup> Unlike the normally developing and regenerating tissues, revascularisation of many rapidly growing tumours, however, is dysregulated and thus markedly erratic as vascularisation does not match the rate and pattern of tumour growth that we found particularly pronounced in the HCC tissue samples. The cell signalling pathways regulating such cell type generation or growth play a critical role but are highly dysregulated in

many tumours including HCC.<sup>10,11</sup> This together with unsustainable tumour size and insufficient blood supply may drive erythrocytic generation without the generation of endothelial cell lining or lack of pericyte/smooth muscle cell recruitment essential for blood circulation.

Cancer represents a dysregulated haphazard pattern of growth characterised by a number of tissue architectural abnormalities. One of the frequent abnormalities observed in such tissues shows the presence of large clusters of blood cells, mainly erythrocytes with a small number of white blood cells, without any sign of blood vessel wall or endothelial cell lining essential for blood circulation. Rapid cancer growth promotes angiogenesis and vascularisation to meet the demands of increased blood supply for rapidly growing tissues. Increased ischaemic stress would also promote haemopoiesis in bone marrow or through recruitment of extramedullary blood supply from spleen under such conditions. Bone morphogenetic protein (BMP) and Hedgehog signalling pathways are known to promote extramedullary haemopoiesis by recruitment of blood cell progenitors from bone marrow to the spleen before arriving in the tumour tissue.<sup>12</sup> The delivery of blood

**Table 1.** PCR primers.

Sulf1	PI3: 5'-TACCCCCATGTGCTGCCCT-3' PI4: 5'-GCCGTGGTCGGCGGTGTAATG-3'	706 bp
Sulf2	PI7: 5'-CAACCGCCTTCTCTCTGCTGGGT-3' PI8: 5'-CTGCAGCATGTTGGTGAAGTCC-3'	805 bp
HIF1 $\alpha$	257: 5'-CGTTCCTTCGATCAGTTGTC-3' 258: 5'-TCAGTGGTGGCAGTGGTAGT-3'	145 bp
EpoR	295: 5'-CTGGTTTGTCCCTGAAGCCT-3' 296: 5'-GATGGGGCTTACAGGGTGT-3'	555 bp
Glycophorin A	281: 5'-TCCGGTGTAACTCTTTCAGGG-3' 282: 5'-CATTGCAGGAGGGTACTCCTT-3'	401 bp
HBA- $\alpha$	279: 5'-GGCGGAGAGGCGCTGGACAG-3' 280: 5'-AACGGTACTTGGAGGTCAGC-3'	351 bp
Hb $\beta/\delta$	293: 5'-CTTTGGGGACCTGTCCACTC-3' 294: 5'-GTCCGGGGACCAAATGACTT-3'	354 bp
PDGFRB	325: 5'-GGCCAGAGCTTGTCTCAAT-3' 326: 5'-AGGGTGGGTTGTCTTTGAA-3'	955 bp
Vegf	a: 5'-GGCAGCTTGAGTTAAACGAAC-3' b: 5'-ATGGATCCGTATCAGTCTTTCCTGG-3'	130 bp
BMPR2	a: 5'-TGGCAGTGAGGTCACTCAAG-3' b: 5'-CACGCCTATTGTGTGACAGG-3'	197 bp
ptc1	321: 5'-TTCGGACCGTATCCTGAGGT-3' 322: 5'-TCTCGCACCGGACGTTAAAA-3'	748 bp
Gli1	323: 5'-ATGTGTGTAAGCTCCCTGGC-3' 324: 5'-CCCCTGCATTGGGGTTGTAT-3'	819 bp
Nanog	283: 5'-GAATAACCCGAATTGGAGCAG-3' 284: 5'-AGCGATTCTTCTTACAGTTG-3'	141 bp
Oct4	285: 5'-ATGTGGTCCGAGTGTGGTTC-3' 286: 5'-GTGGTGACAGACACAGAGGG-3'	241 bp
Bcl2	287: 5'-TGGATGACTGAGTACCTGAA-3' 288: 5'-GGCCTACTGACTTCACTTAT-3'	206 bp
Bax	289: 5'-CGAATGTCTCAAGCGCATCG-3' 290: 5'-TTCCAGATGGTGAGTGACGC-3'	387 bp
$\beta$ -actin	P0: 5'-CTATGAGCTGCCTGACGGTC-3' P00: 5'-AGTTTCATGGATGCCACAGG-3'	114 bp

PCR: polymerase chain reaction.

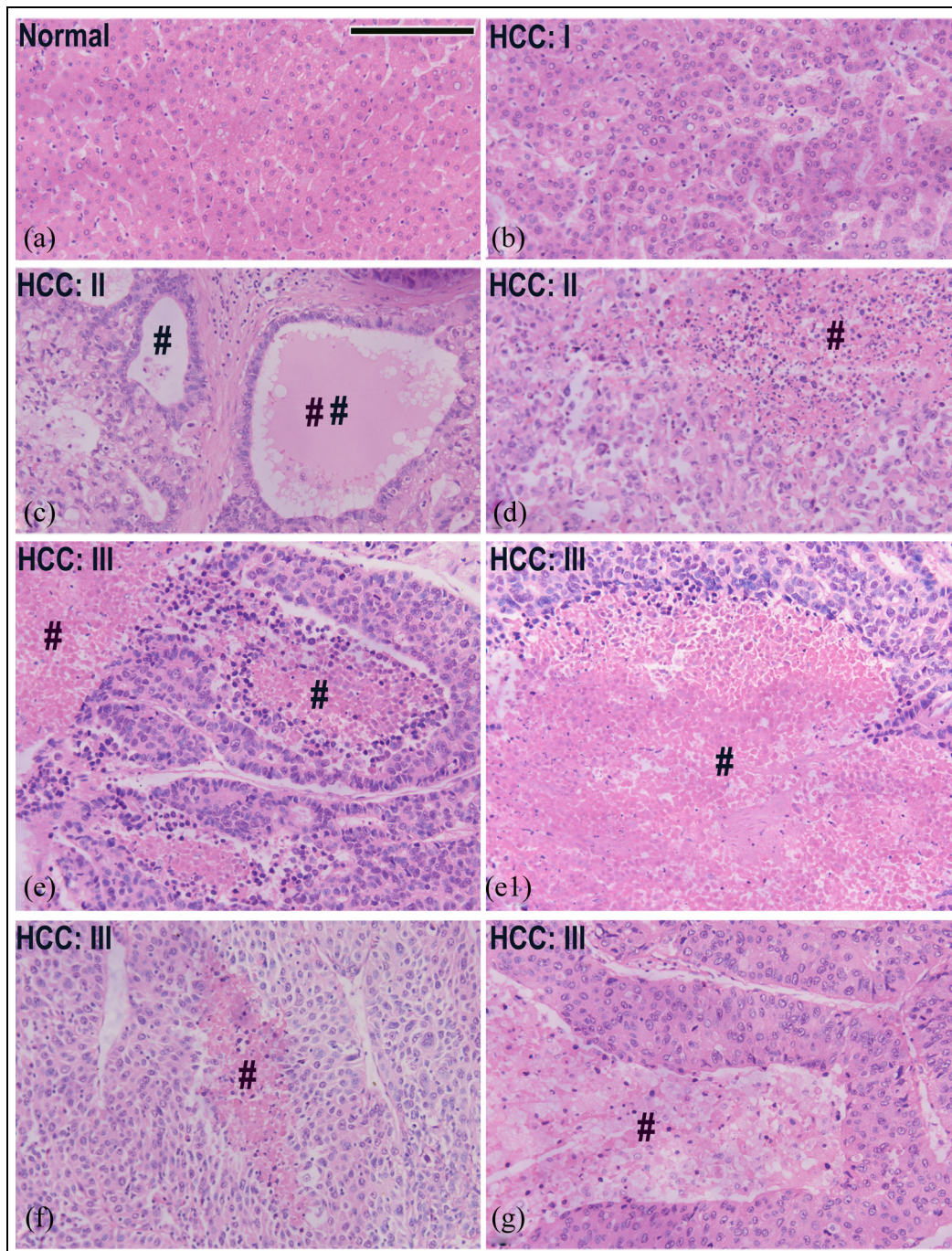


**Figure 1.** H&E-stained paraffin sections of normal human liver and hepatocellular carcinoma tissues at different stages of disease: (a) normal (liver sample from a 66-year-old male), (b) HCCI (liver sample from a 42-year-old male), (c) HCCII (liver sample from a 43-year-old male), (d) HCCII (liver sample from a 62-year-old male), (e) and (e1) HCCIII (liver sample from a 63-year-old male), (f) HCCIII (liver sample from a 38-year-old male) and (g) HCCIII (liver sample from a 55-year-old male). Symbol # indicates areas showing the presence of a large proportion of non-nucleated cells or death of such cells (##). Areas labelled with symbol # in (d), (e), (e1), (f) and (g) clearly indicate gradual loss of nuclei as is apparent from the elimination and shrinking nuclear morphology. The arrangement of these cells without any clear borders also excludes the possibility of these cells resulting from bleeding or through extramedullary haemopoiesis. Scale bar = 100  $\mu$ M.

supply from both the bone marrow and/or spleen, however, is dependent on the establishment of blood vessel channels that are also essential for transport to and

from the lungs. The lack of well-developed, or even poorly developed, endothelial lined channels surrounding blood clusters, in a number of tumour tissues,

prompted us to hypothesise that such blood cell clusters that were very common in canine HCC samples did not arrive from the bone marrow or the spleen, but were a result of in situ cancer stem cell fate change triggered by dysregulated growth associated ischaemia. The key objective of this study therefore was to determine if HCC cells in such regions demonstrated any signs of transdifferentiation into erythrocytes. This was supported by our observations that not all such erythrocytic cells were fully differentiated but included a number of cells in the process of nuclear exclusion or necrosis without any defined borders as erythrocytes normally differentiate and extrude nuclei in bone marrow before entering circulation. We therefore investigated if certain regions of cancer tissue exhibited hypoxia or signs of stem cell fate change to erythrocytic cell type characteristics. The ischaemic nature of the cancer tissue was examined by the activation of HIF1 $\alpha$  triggering the activation of the erythropoietin receptor. The change in stem cell fate of hepatocyte to erythrocyte was examined by double immunofluorescence procedure showing the presence of Glycophorin A, an erythrocytic progenitor marker, and the presence of a hepatocytic marker called cytokeratin 18 in the same cell.<sup>13</sup> The generation of erythrocytic clusters in such HCC regions was further confirmed by activation of additional known stem cell markers such as NANOG and OCT4 with Glycophorin A in the same cell.

This study thus demonstrates the presence of a large number of blood cell clusters without any blood vessel walls that ultimately undergo apoptosis, resulting from a change in the hepatocytic cell fate. This was confirmed not only by the in situ activation of, for example, OCT4 and Glycophorin A but also by detection of haemoglobin synthesis, the levels of which can be further modulated by changes in Sulf1/Sulf2 and multiple cell signalling pathways. The lack of blood vessels around such erythrocytic cell clusters that leads to premature apoptosis without benefitting any tissue highlights further metabolic stress in such tumours.

## Materials and methods

### Tissue histology and immunocytochemistry

All canine (50 samples) and feline (10 samples) tumour tissue sections of formalin-fixed tissues in the age range of 8–11 years and their clinical history were provided by the RVC diagnostic laboratory following an RVC ethical approval. All human HCC tissue arrays (87 samples) were purchased through US Biomax. Unlike the human tissue arrays, a large majority of the animal tissue samples were large biopsies often exceeding 2.5 cm in length and width. Some tissue samples also included two to three biopsies from different regions of the same liver. All such biopsies included both tumour

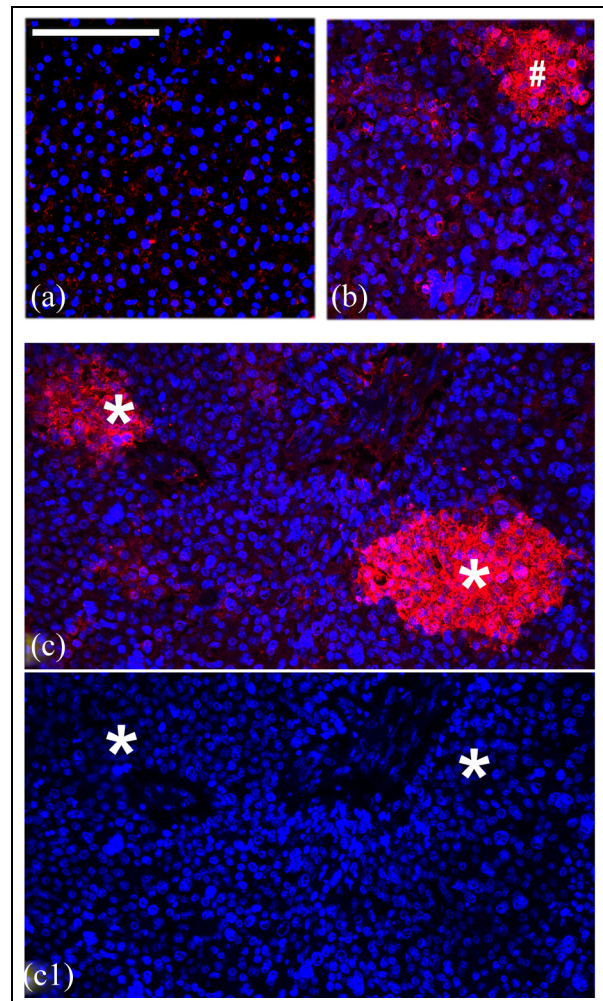


**Figure 2.** A liver sample from normal human (a) and two HCCIII human liver sample (b) and (c) sections immunostained for active caspase 3 (red) enzyme and superimposed with nuclear DAPI (4',6-diamidino-2-phenylindole) stain (blue) to determine if certain cells were undergoing active apoptosis. Red fluorescence shows the presence of active caspase 3. Section (c1) represents DAPI stain alone for section (c) as nuclear stain can be seen more clearly without being partly masked by caspase stain. Scale bar = 100  $\mu$ M.

and small proportions of unaffected cells in the distant regions of the same biopsy. Tissue sections for morphological observations were stained with a standard haematoxylin and eosin stain. Double immunofluorescent procedure as described previously<sup>14</sup> was used to evaluate the cellular phenotypes of normal and 15 HCC tissues. Following commercial antibodies were used for this analysis: Wnt2 (Prestige)-1/150, active caspase-3 (R&D)-1/100, ptc1 (Millipore)-1/300, p-Smad1,5,8 (Cell signalling)-1/300, HIF1 $\alpha$  (Novus)-1/40, EpoR (Abcam)-1/250, Glycophorin A (Abcam)-1/10, Cytokeratin 18 (Abcam)-1/300, smooth muscle  $\alpha$ -actin (IA4)-1/400, vWF<sup>15</sup> (Dako)-1/200, rabbit anti CD146

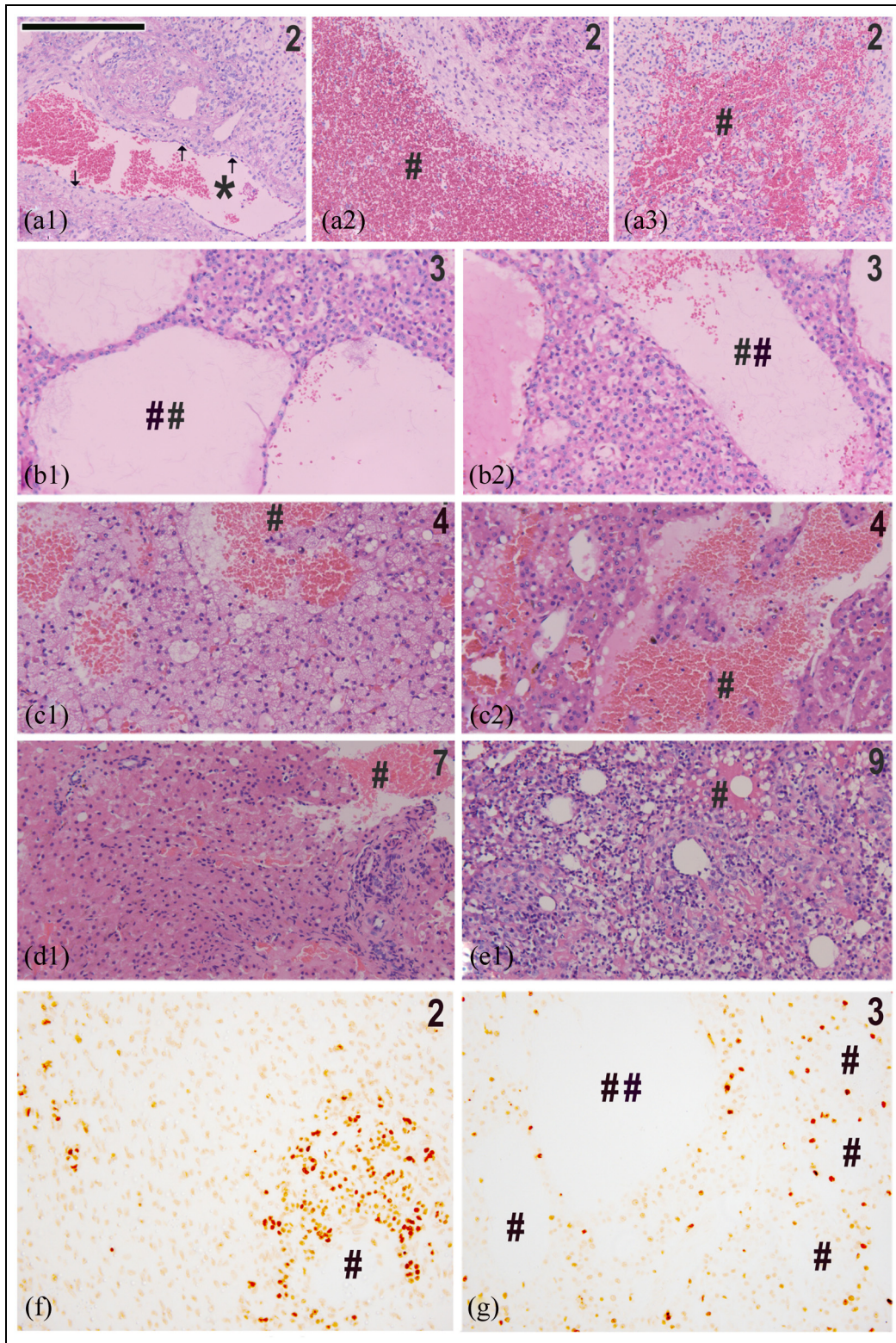


**Figure 3.** (a)–(e) H&E staining of HCC samples from different regions of the same canine patient or different canine (a1)–(d1) patients that ranged from 8 to 11 years of age (e.g. (a1)–(a3) = patient 2, (b1) and (b2) = patient 3, (c1) and (c2) = patient 4, (d1) = patient 7 and a feline patient (e1) = patient 9). The numbers 2–9 in the top right-hand corner refer to the patient number used for molecular analyses in Figures 8 and 9. (f) and (g) TUNEL stain of some such HCC canine liver tissue sections (patients 2 and 3) to demonstrate apoptosis and or eventual necrosis of such cells. Very clear demonstration of non-nucleated cells not appearing as a result of bleeding or by extramedullary haemopoiesis is also apparent in (a3) that shows the interdigitation of these cells with the nucleated cells. Scale bar = 100  $\mu$ M.

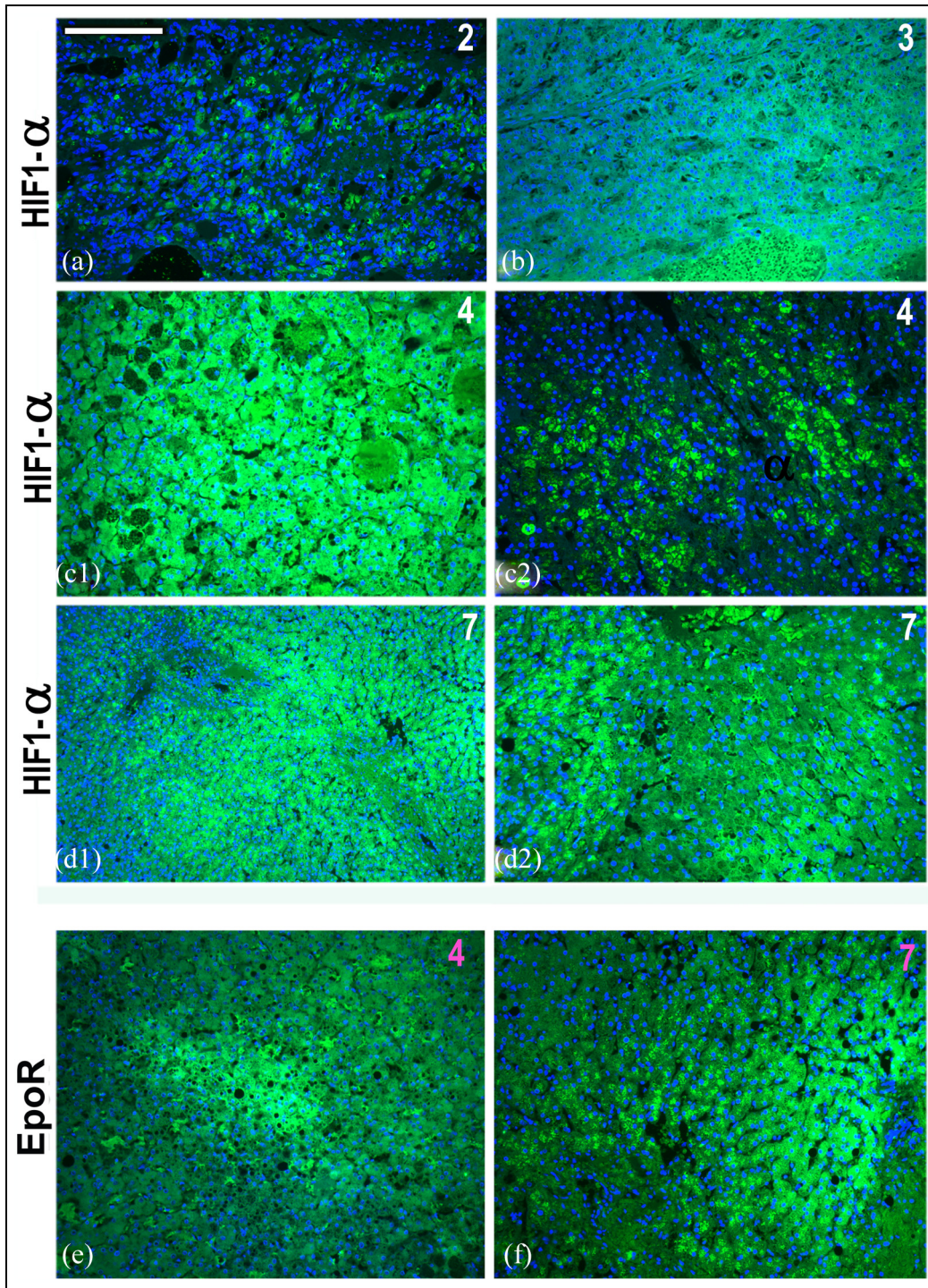


**Figure 4.** (a)–(d) HCC liver tissue sections from different patients ((a) = patient 2, (b) = patient 3, (c1) and (c2) = patient 4, (d1) and (d2) = patient 7) stained with antibody to HIF1 $\alpha$  by immunofluorescence. Samples (e) (patient 4) and (f) (patient 7) are stained for EpoR by immunofluorescence. Scale bar = 100  $\mu$ M.

(Sigma)-1/200, mouse anti NANOG (Abcam)-1/100 and rabbit anti OCT4 (Novus biologicals)-1/100. With the exception of Glycophorin A antibody that itself is linked to 488 fluorochrome, the binding of all other antibodies was detected by secondary antibodies linked

to 488 (green) fluorochrome or 594 (red) fluorochrome as previously described.<sup>14</sup> Immunoperoxidase staining was used to detect the expression pattern of active- $\beta$ -catenin (Millipore) antibody using 1/100 dilution as previously described.<sup>16</sup>

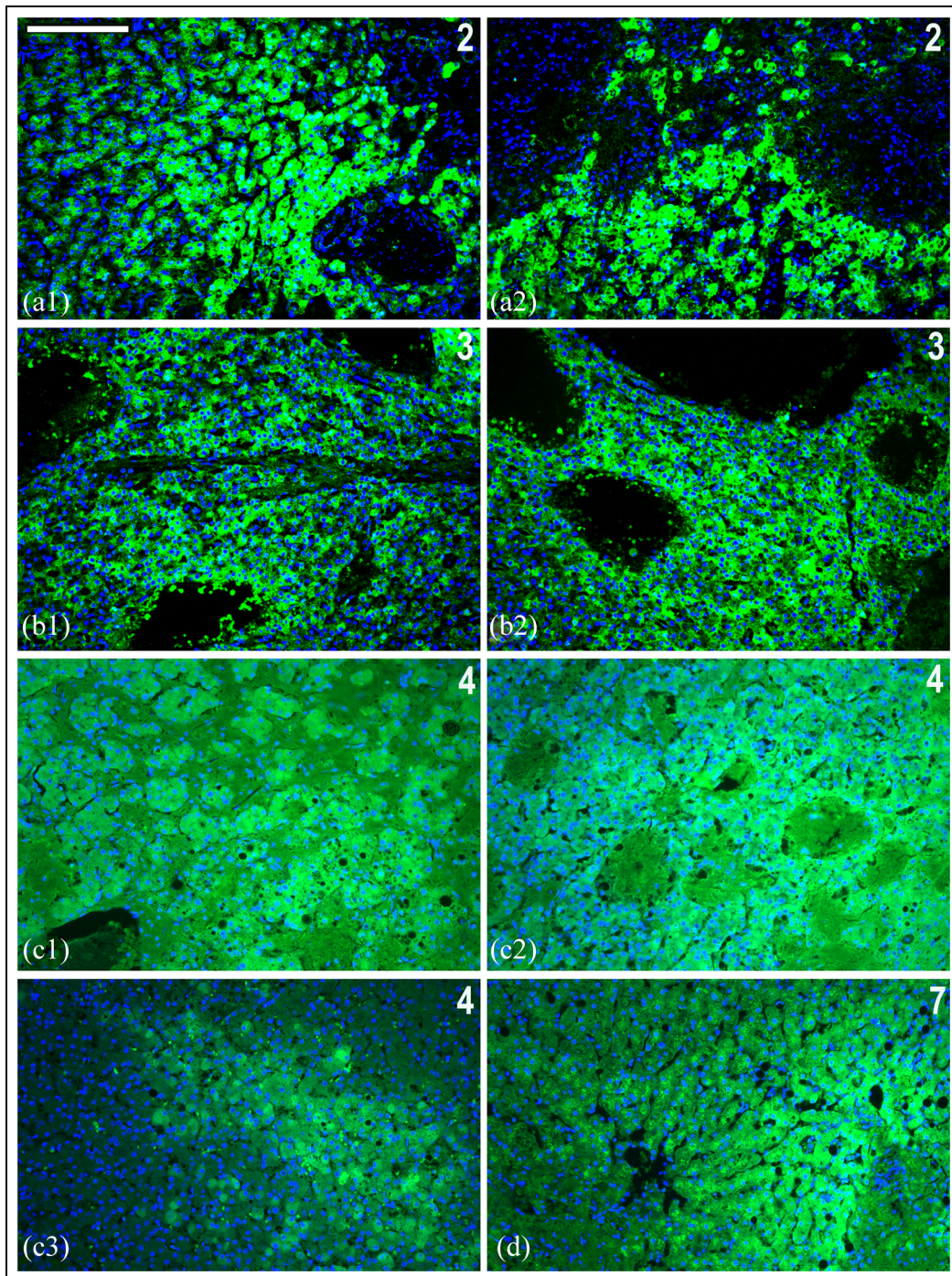


**Figure 5.** (a)–(d) HCC liver tissue sections from different patients ((a1) and (a2) = patient 2, (b1) and (b2) = patient 3, (c1)–(c3) = patient 4, (d) = patient 7) stained with antibody to Glycophorin A, an erythroid marker by immunofluorescence. Scale bar = 100  $\mu$ M.

#### *Reverse transcription polymerase chain reaction*

All 50 canine and feline tumour tissues and normal or unaffected liver samples for reverse transcription polymerase chain reaction (RT PCR) analysis were supplied by the RVC bio-bank following owner informed consent and RVC ethical approval. All these tissue samples

were used to prepare total RNA using Trizol to generate complementary DNA (cDNA) with reverse transcriptase as described previously.<sup>17,18</sup> Only 10 HCC tumour biopsies for which we also had detailed immunocytochemical analysis were selected for further RT PCR analysis. The polymerase chain reaction (PCR) of

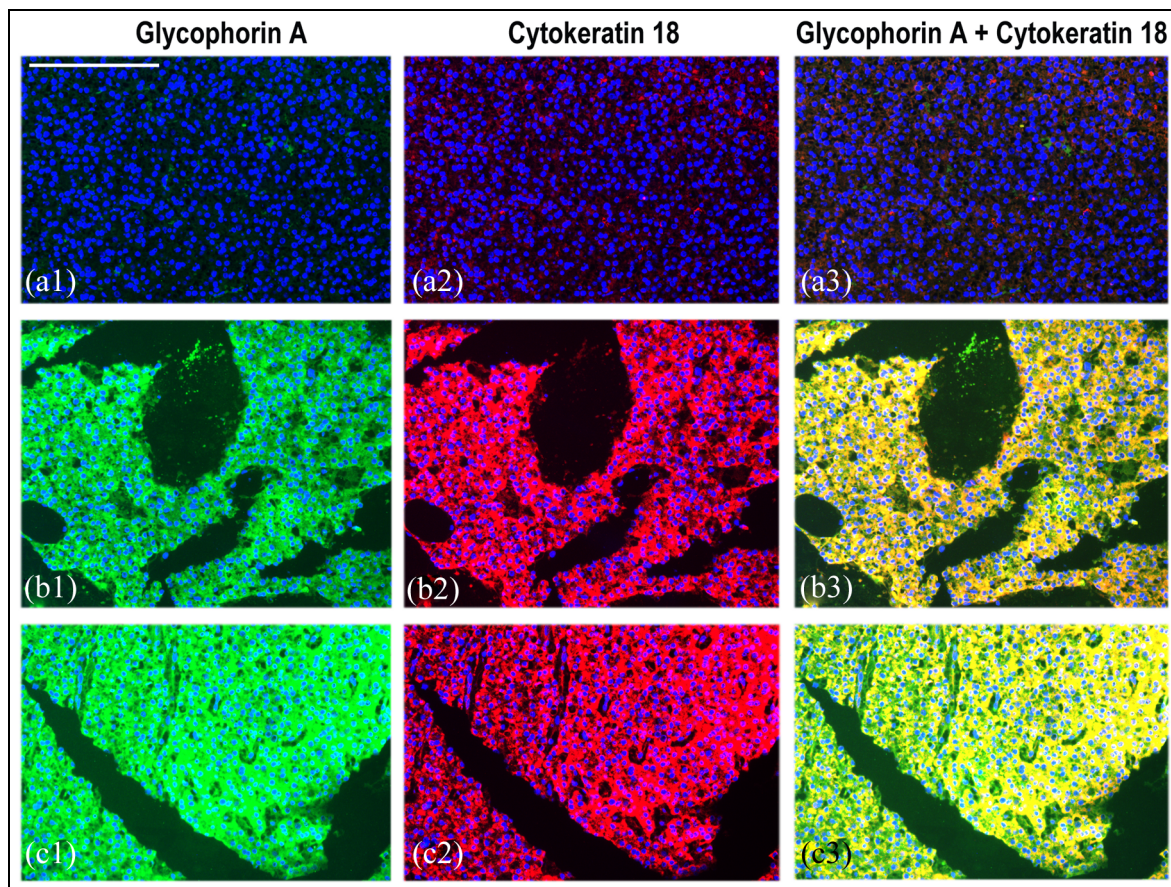


**Figure 6.** The expression of Glycophorin A, an erythroblast marker and cytokeratin 18 associated with HCC tumours is undetectable in normal and unaffected adjacent regions of canine liver ((a1), (b1) and (c1)) while both Glycophorin A ((b1) and (c1)) and cytokeratin 18 ((b2) and (c2)) at variable levels were detected in the same cells ((b3) and (c3)) in a large proportion of the HCC tumours undergoing transdifferentiation (detected by double immunofluorescence procedure). Scale bar = 100  $\mu$ M.

such samples was carried out using canine/feline primers listed in Table 1. PCR fragments following 40 amplification cycles were photographed following separation in 2% agarose gels.

## Results

### *The presence of erythrocyte-like cell clusters in HCC*

The normal liver is composed of single-layered hepatocyte cords separated by sinusoids (Figure 1(a)). This highly organised structure is disrupted in HCC-afflicted livers (Figure 1(b)–(g)) as shown in the H&E-stained human liver sections. These human HCC livers show not only the histopathological changes characterising HCC but also additional changes highlighting the presence of non-nucleated erythrocyte-like cells without any endothelial cell lining or blood vessel walls. Such non-nucleated erythrocyte-like clusters highlighted by symbol # also show the presence of a number of cells with reduced nuclear stain, indicating the gradual in situ generation of non-nucleated cells from nucleated basophilic

cells rather than recruitment from the bone marrow. The non-nucleated eosinophilic clusters of cells (indicated by #) were often surrounded by basophilic cells (Figure 1(e)). Non-nucleated cell clusters often eventually led to necrosis (indicated by # #) and thinning out of solid tumour in some places (Figure 1(c)). Loss of nuclei and localised apoptosis was also apparent in some human HCC samples detected by antibody staining of active caspase 3 (Figure 2). Immunofluorescent staining with most antibodies also highlighted high levels of erythrocytic autofluorescence at earlier stages that was reduced during later necrotic stages.

The abundance of non-nucleated cells among HCC cells was further investigated by H&E staining (Figure 3(a1)–(e1)) of some canine and feline HCC livers and all further work was restricted to canine and/or feline tissue samples as we also had some matching fresh tissue samples for RT PCR. The presence of non-nucleated irregular erythrocyte-like clusters (highlighted with symbol #) without any endothelial cell lining appeared even more apparent in many canine and

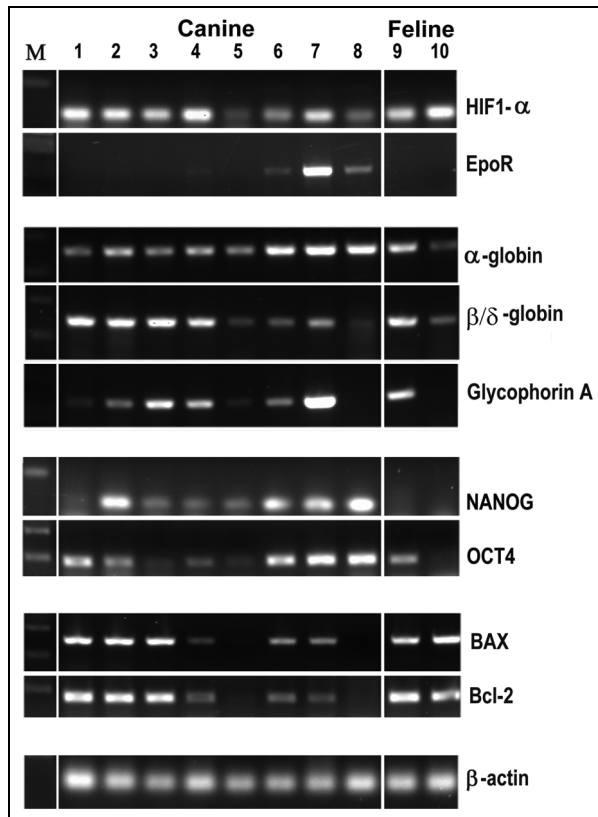


**Figure 7.** The detection of mRNAs representing hypoxia, erythroblast/erythrocyte markers, stem cell markers and apoptotic/anti-apoptotic in 10 different canine HCC tissues using RT PCR analysis. None of the control tissues showed the expression of any detectable levels of these markers (not shown).

some feline HCC livers. This differed from the erythrocytes present in normal blood vessels (\*) bounded by endothelial cell lining (indicated by the arrows in Figure 3(a1)). A TUNEL (terminal deoxynucleotidyl transferase (TdT) dUTP nick-end labelling) assay, which detects DNA fragmentation with TUNEL, detected the presence of a number of cells undergoing apoptosis and cell death leading to complete loss of large clusters of cells in such HCC canine liver samples (Figure 3(b1), (b2) and (g)).

### Evidence of ischaemia in HCC tissues

Since several regions of apoptosis/necrosis, often associated with non-nucleated erythrocyte-like clusters, were observed in some human and many canine HCC livers, we examined if such changes resulted from ischaemia due to sinusoidal occlusion. This was checked by antibody staining for hypoxia-inducible factor 1-alpha (HIF1 $\alpha$ ) that is considered to be a master transcriptional regulator of cellular hypoxia. Unlike the normal

liver (not shown), many HCC liver samples showed variable levels of HIF1 $\alpha$  in localised regions. Further staining of such tissues also showed the presence of the erythropoietin receptor (EpoR) protein (Figure 4) known to be expressed only transiently, in localised regions of HCC but not the normal liver.

### Presence of multiple erythrocytic markers in HCC liver cells without blood vessel markers

The HCC and normal liver tissue sections were also stained with an antibody to Glycophorin A (an erythroid-lineage-specific membrane sialoglycoprotein) to determine if hypoxia or ischaemia induces in situ generation of erythroid cells in such tissues as indicated by the presence of many non-nucleated cells. Glycophorin A is an erythrocytic membrane protein expressed at all stages of erythroid differentiation that includes both nucleated and non-nucleated stages of differentiation. This study detected localised presence of Glycophorin A only in certain regions of nucleated HCC liver cells (Figure 5). The transdifferentiation of HCC hepatocytes into erythrocytes was further indicated by the co-expression of Glycophorin A, an erythroid marker, and cytokeratin 18, a hepatocytic marker, that is also described as an epithelial cancer stem cell marker, in a subset of cells resembling hepatocytic cords in a number of HCC patient samples (Figure 6).

The HCC hypoxia was further confirmed by RT PCR analysis of HIF1 $\alpha$  and EpoR messenger RNAs (mRNAs) in such samples as was the presence of a number of erythrocytic mRNAs detected by RT PCR in eight canine (1–8) and two feline (9 and 10) HCC liver samples (Figure 7). Erythrocytic markers analysed by RT PCR in this study included Glycophorin-A,  $\alpha$ -globin and  $\beta/\delta$ -globin. Such HCC liver sample analysis also showed the presence of NANOG and OCT4 stem cell markers indicating their potential to transdifferentiate into other cell types such as erythrocytes. Also detected in these samples was the mRNA for BAX and bcl-2, pro-apoptotic and anti-apoptotic markers.

The presence in normal liver but absence of blood vessels around erythrocytic clusters in HCC samples was confirmed by staining for vWF,<sup>15</sup> an endothelial cell marker and for smooth muscle  $\alpha$ -actin, a smooth muscle cell marker and another blood vessel marker called CD146 (Figure 8). These antibodies stained blood vessel lining in normal and unaffected adjacent regions but not around such cell clusters in HCC tissues although remnants of some endothelial cell lining (indicated by shrunken irregular cell shapes and small fragments of membranous component) could be detected in some regions.

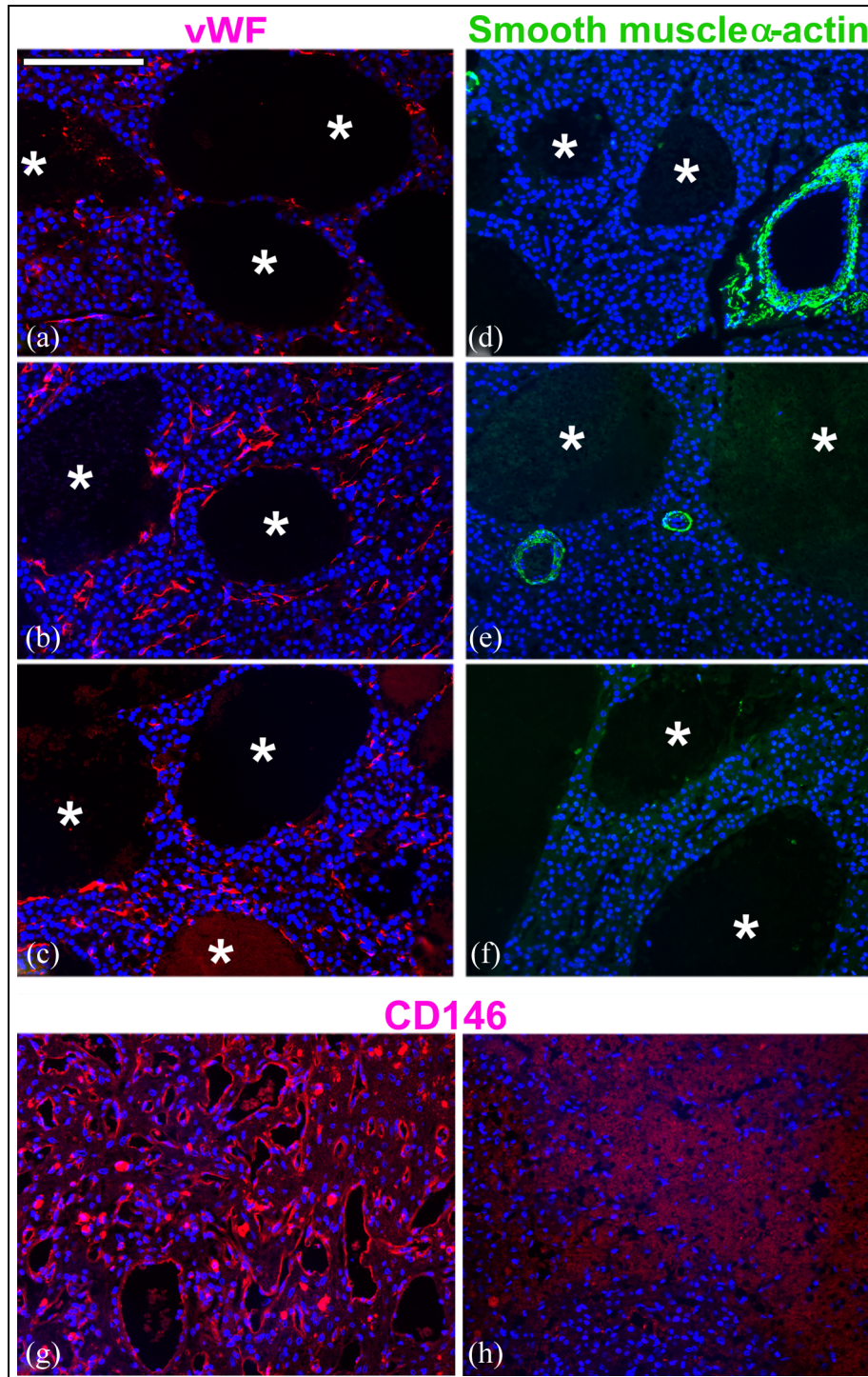


**Figure 8.** Staining of canine HCC patients 2 (a) and (d) and patient 3 (b), (c), (e), (f) livers for vWF (a)–(c) and smooth muscle  $\alpha$ -actin (d)–(f) using immunofluorescence procedure. \*Highlights the areas with remnants of erythrocytes without any endothelial (vWF) or smooth muscle cell lining (smooth muscle  $\alpha$ -actin). The presence of blood vessels/sinusoids in an unaffected normal canine liver (g) compared with non-detection of any blood vessels in HCC canine patient 2 (h) is also apparent from the staining for CD146 antigen regarded as an essential component of blood vessels as it stains endothelial cells. Scale bar = 100  $\mu$ M.

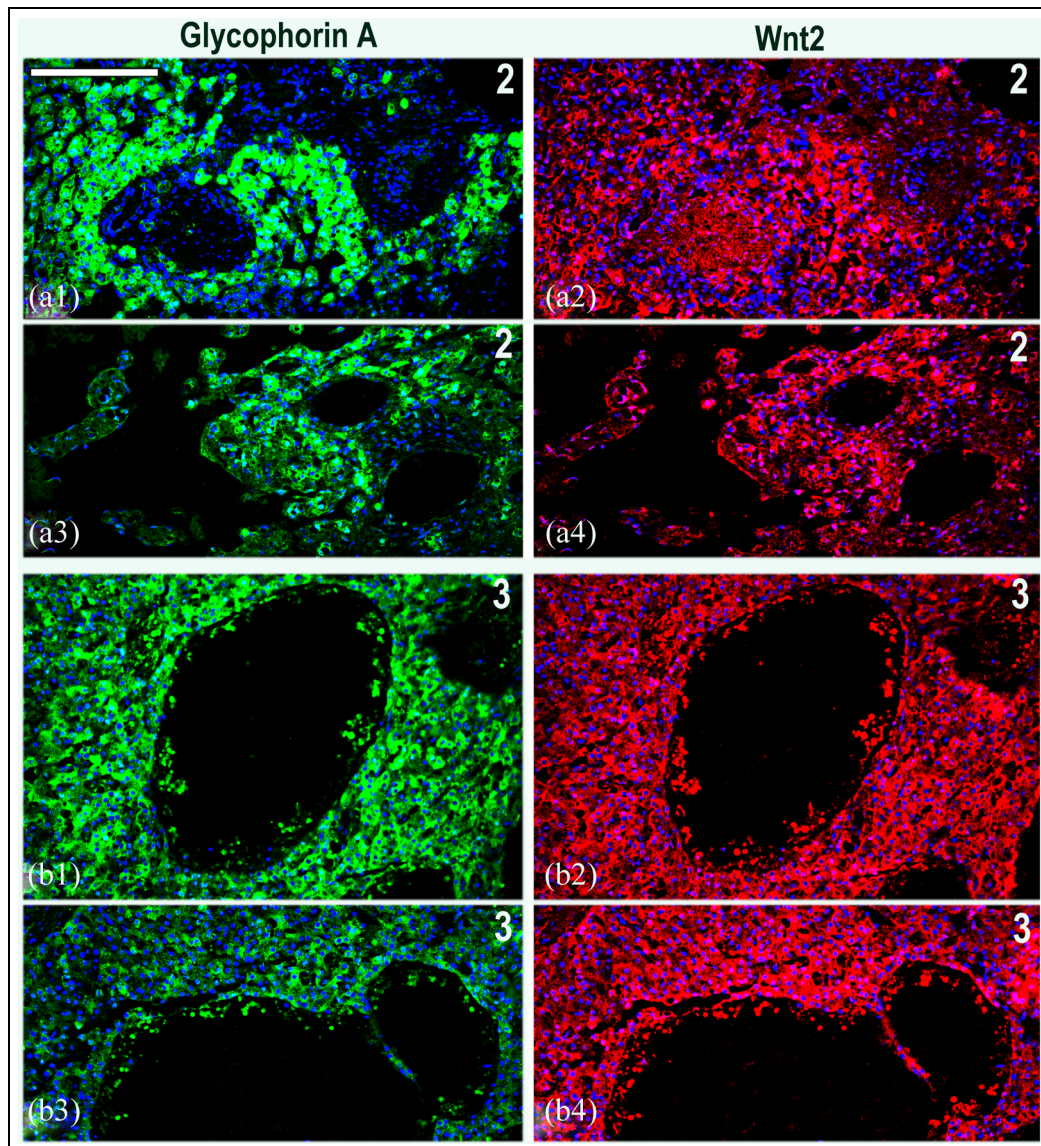


**Figure 9.** Double immunofluorescence staining of different regions of patient 2 (a1)–(a4) and patient 3 (b1–b4) liver samples for the expression of Glycophorin A (green) and Wnt2 ligand (red) in epithelial-like hepatocytes indicates possible involvement of Wnt signalling in cellular transdifferentiation. Scale bar = 100  $\mu$ M.

### *Activation of multiple cell signalling pathways in HCC liver tissues*

Since Wnt signalling is known to promote erythroid differentiation, we first examined the expression of Wnt2 ligand in HCC samples to see if Wnt2 expression correlated with areas of Glycophorin A expression. The double immunofluorescence for these two markers showed close correlation of Glycophorin A expression with the expression of Wnt2 ligand in nucleated cells of a number of HCC patients (Figure 9) indicating Wnt signalling involvement in erythroid specification or differentiation. The presence of Wnt signalling indicated by the detection of Wnt2 ligand in HCC livers was

further examined by the staining for active- $\beta$ -catenin translocation into nucleus in such samples. A significant proportion of HCC cells in such tissues demonstrated activated- $\beta$ -catenin in the nuclei (Figure 10(a)–(c1)) that is a key downstream transcriptional co-activator of canonical Wnt signalling. The size of the activated- $\beta$ -catenin (brown)-positive nuclei was nearly twice the size of the unstained blue nuclei of unaffected cells in such samples. Wnt signalling, however, was not the only cell-signalling pathway active in such cells. Immunocytochemical analysis showed the activation of sonic hedgehog (SHH) signalling, apparent from the recruitment of its receptor, ptc1, as was the activation of both Sulf1 and Sulf2 mRNA (Figure 11) that are

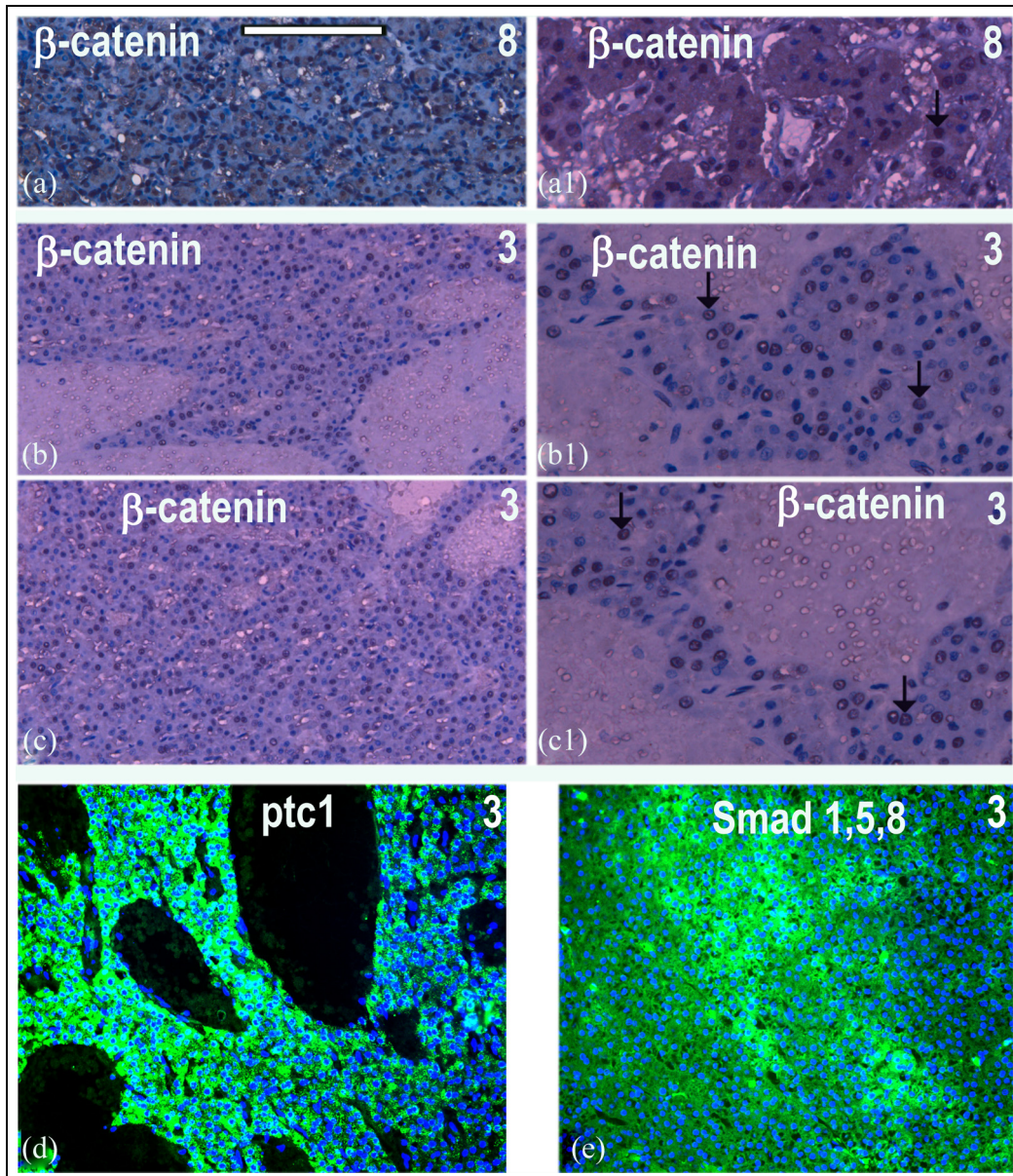


**Figure 10.** The staining for the expression of active nuclear  $\beta$ -catenin by immunoperoxidase followed by H&E stain is shown at low magnification (a)–(c) and higher magnification of patient 8 (a) and (a1) and different regions of tissue samples from HCC patient 3 (b), (b1), (c) and (c1) further indicating the involvement of canonical Wnt signalling. SHH signalling is examined by immunofluorescent staining for ptc1 (d) while BMP signalling was examined by immunofluorescent staining for Smad 1,5,8 (e). Scale bar = 100  $\mu$ M.

usually undetectable in the normal adult liver.<sup>17,18</sup> The activation of SHH signalling was also confirmed by the activation of ptc1 and Gli mRNA using RT PCR analysis. BMP signalling was also apparent from the detection of its Smad1,5,8 downstream targets detected by immunocytochemistry (Figure 10(d) and (e)) as well as by the detection of BMP2 mRNA (Figure 10). Also detected in these HCC tissue samples was the presence of vascular endothelial growth factor (VEGF) ligand and PDGFR-B receptor mRNA (Figure 11) thus showing the activation of multiple cell signalling pathways.

#### *Activation of stem cell markers in HCC regions undergoing transdifferentiation*

To further confirm cancerous hepatocytic transdifferentiation into erythrocytes and to ascertain the activation of stem cell markers indicated by RT PCR analysis of canine HCC samples, this study was further extended by immunocytochemical analysis of OCT4, NANOG and CD146. CD146 normally associated with blood vessels has also been reported to be a stem cell marker in some cancer tissues. NANOG and OCT4 (Octamer-binding transcription factor 4) are known to be key

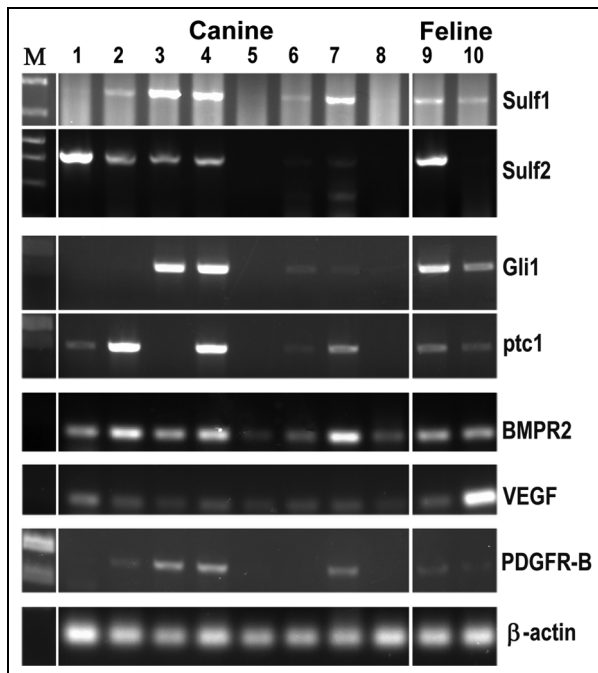


**Figure 11.** The detection of different cell signalling components in 10 different canine HCC tissues using RT PCR analysis. None of the controls showed the expression of Sulfl/Sulfl2 or any detectable levels of such cell signalling components (not shown).

regulators of embryonic stem cell self-renewal and pluripotency with a potential to re-activation in cancer. CD146 expression is generally restricted to blood vessels in normal liver (Figure 8(g) and 12(a2)), but its expression was observed in certain regions of hepatocyte-like cancer cells (Figure 12(b)–(d)). While OCT4 and NANOG expression could easily be identified in embryonic tissues (Figure 12(e) and (f)), these transcription factors were undetectable in normal unaffected liver (Figure 12(g) and (h)). The expression of NANOG using this antibody was generally low in the HCC samples tested (Figure 12(i)), but the nuclear expression of OCT4 was clearly apparent in a number of cells in the areas adjacent to erythrocytic clusters (Figure 12(j)–(l)). The proportion of cells expressing OCT4 in such samples showed marked regional differences that ranged from 0% to moderate levels of 5%–18% but exceeding 95% in some other areas (Figures 12 and 13). The level of OCT4 expression in individual cells was also variable ranging from barely detectable levels to high level of expression (Figures 12 and 13). Level of OCT4 expression did not only vary in the nucleus but was also observed in the cytoplasm in some regions as this transcription factor is known to shuttle between nucleus and cytoplasm.<sup>19</sup>

Double immunofluorescence procedure confirmed close correlation of OCT4 and Glycophorin A

expression in the same cell undergoing hepatocytic to erythrocytic transdifferentiation (Figure 13) although the levels of both these markers varied during different stages of such change.

## Discussion

HCC, like many other cancers, undergoes marked histopathological changes disrupting normal cell function. However, it was unusual to see large clusters of erythrocytes without any endothelial cell lining or blood vessel walls in a number of HCC tumour tissues. While the number of such erythrocytic clusters was small in human tumours, such cells were much more abundant and apparent in many canine HCC cancers. The erythrocytic identity of such cells could easily be ascertained by the absence of nuclei using both general histological stains and morphological changes observed by DAPI (4',6-diamidino-2-phenylindole)-stained nuclei. Indeed, the presence of large pools of blood containing differentiated erythrocytes was even apparent by red haemoglobin in a number of unstained HCC tumour sections. The generation of such cells could be triggered by tissue hypoxia,<sup>20</sup> a pathophysiologic property of many cancers that is indicated by the activation of HIF1 $\alpha$  transcription factor in certain regions of most HCC tissues. Ischaemia is further highlighted by the detection of EpoR in a number of HCC tissues though not all since erythropoietin (Epo), a key haemopoietic cytokine, induced by hypoxia is expressed only transiently but controls erythropoiesis and protects cells from hypoxic damage.<sup>21</sup> Primary role of Epo signalling is thus to promote proliferation of erythroid progenitor cells and rescue erythroid progenitors from cell death.

Many tissues and particularly liver also have the capacity to generate blood cells outside the bone marrow not only during normal development but also during chronic anaemia or stress<sup>22</sup> as is a feature of many cancer tissues. Erythrocytic cells in these HCC tumours, however, clearly did not arise by extramedullary haemopoiesis (EH), a process that sometimes is triggered by stress as a compensatory mechanism. EH requires blood circulation and thus the presence of blood vessels. The presence of non-nucleated erythrocyte-like cell clusters at different stages of differentiation without any evidence of surrounding blood vessels or endothelial cell lining thus raises the question of the origin of such cells. The alternative explanation therefore is the transdifferentiation of hepatocytic cancer/stem cells into erythrocytes as indicated by the appearance of Glycophorin A in epithelial cells resembling hepatocytic cords before adopting mesenchymal state. This conclusion was further supported by evidence of localised hypoxia, its downstream targets and activation of a number of cell signalling pathways associated with

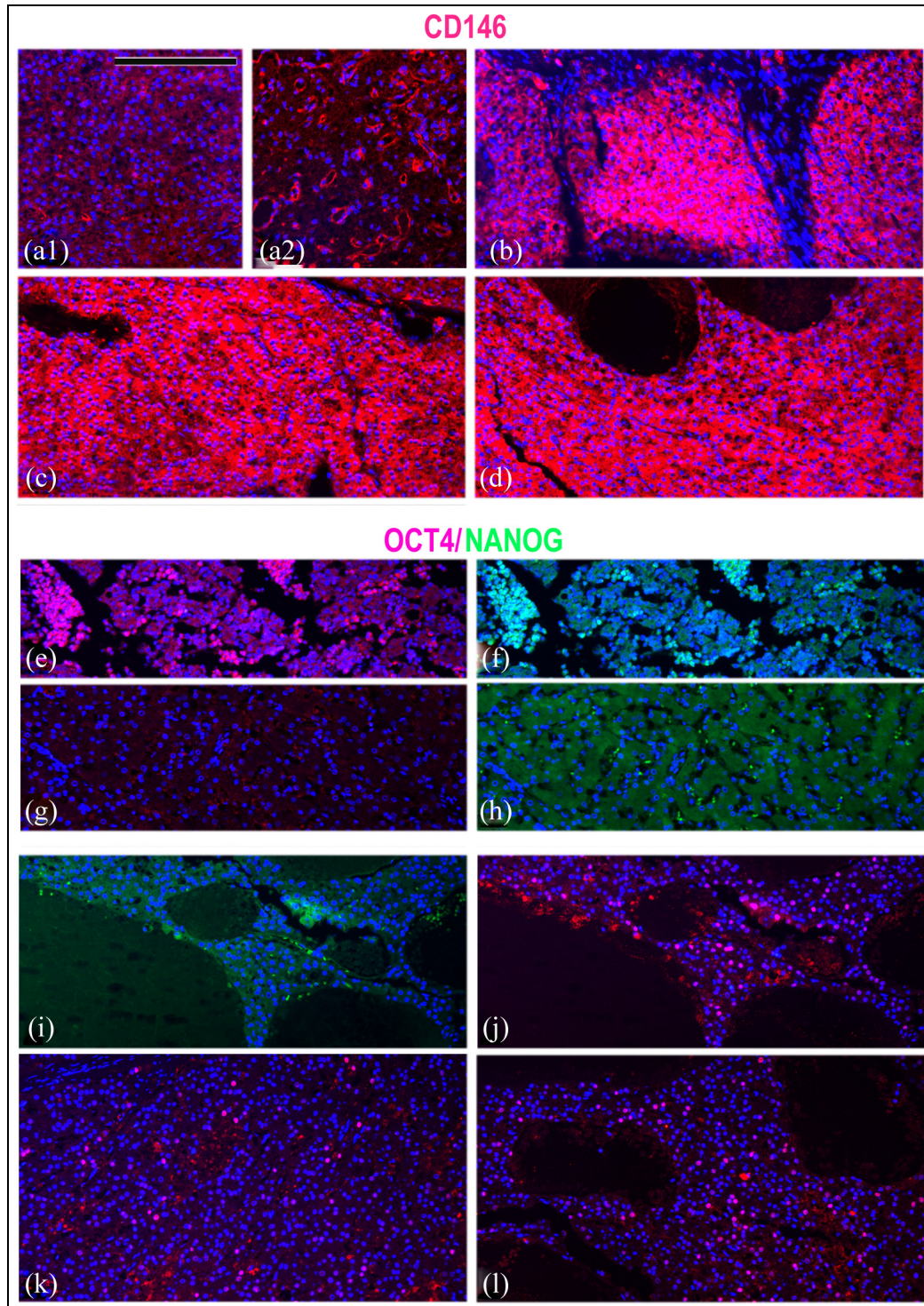


**Figure 12.** The expression of CD146, NANOG and OCT4 proteins was analysed by antibody staining to determine if HCC livers undergoing transdifferentiation were activating some stem cell markers. CD146 expression in two regions of unaffected control liver (a1) and (a2) and HCC livers (b–d) from patients 3, 2 and 1 was analysed using immunofluorescence. The activity of antibodies to OCT4 and NANOG was ascertained by their staining of normal CS18 human embryonic tissue (e and f) that showed no staining of normal or adjacent canine liver (g and h). Double immunofluorescence staining of patient 3 liver shows much higher expression of OCT4 in a selected sub-set of cells when compared with NANOG expression (g). OCT4 was always detectable near regions showing different developmental stages of erythrocytic cluster formation (i–l) in such livers. Scale bar = 100  $\mu$ M.

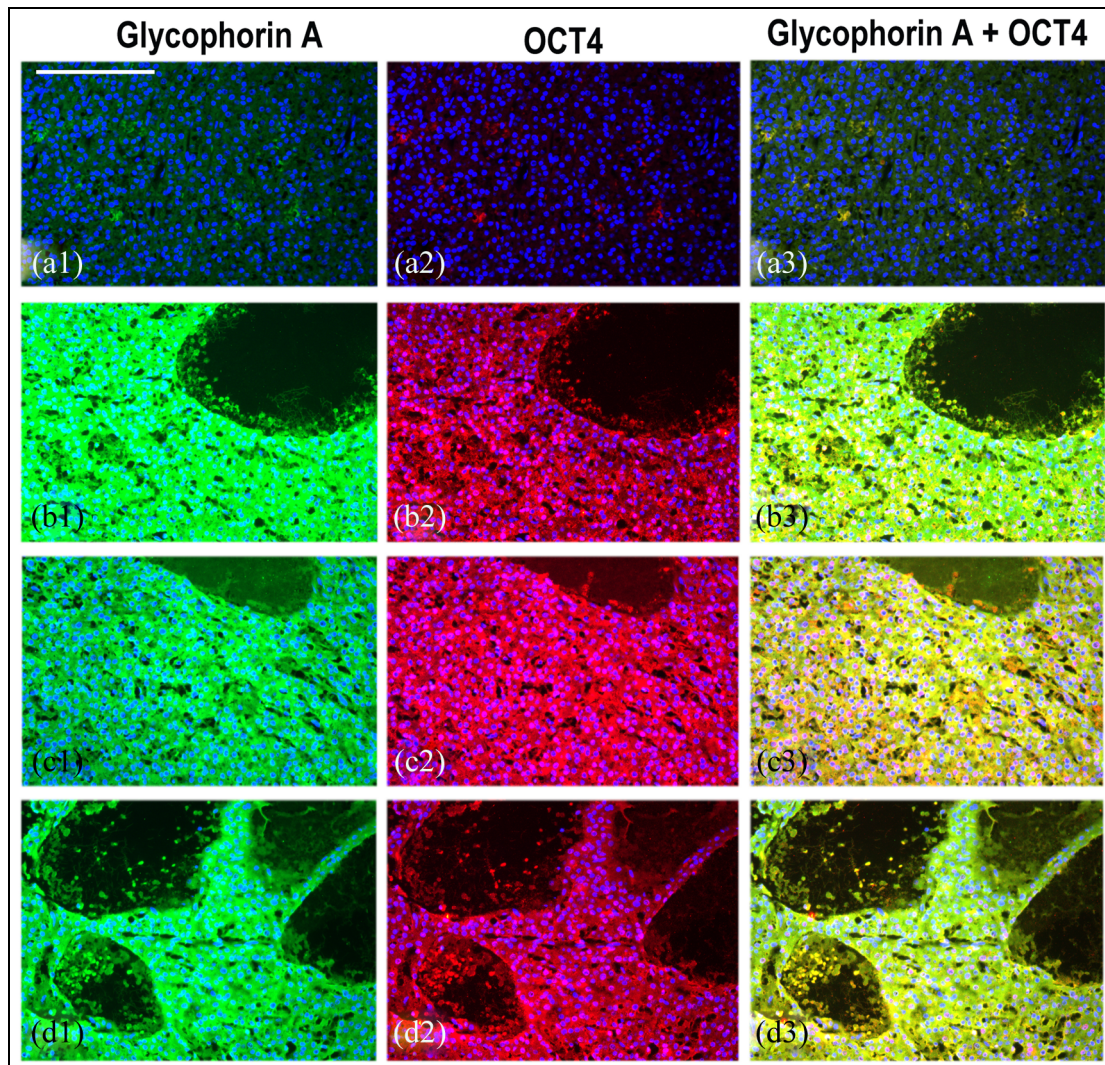


**Figure 13.** The expression of Glycophorin A and OCT4 is undetectable in normal and adjacent unaffected canine liver (a1–a3) but both these markers are co-expressed in a large proportion of the HCC livers in many regions. (b1)–(b3) and (c1)–(c3) represent two different regions of canine patient 2 while (d1–d3) represents HCC liver from canine patient 3. OCT4 transcription factor shows both nuclear and cytoplasmic expression in these regions of HCC livers (b2, c2 and d2). Scale bar = 100  $\mu$ M.

erythropoiesis as well as by co-expression of cytokeratin 18 and Glycophorin A in the same cell.

Most cancer tissues show the existence of stem cell subpopulations that keep the cancer growth going and often persist following drug treatment. Activation of stem cell-like characteristics enables such cells to change cell fate as and if required under hypoxia and associated stress. The presence of stem cell-like cells in the current analysis of canine HCC tumours was apparent from the detection of NANOG and OCT4 transcription factors that regulate self-renewal and pluripotency.<sup>23</sup> Such stem cells therefore have the potential to undergo erythropoiesis and/or angiogenesis. Erythropoiesis is triggered by hypoxia that these tissues clearly experience and induce erythropoietin activation as revealed by the detection of EpoR. The activation of erythrocytic markers in most

canine HCC tumours was apparent using immunocytochemical (Glycophorin A) and RT PCR analyses of mRNAs for  $\alpha$  and  $\beta/\delta$  haemoglobins. The activation of erythropoietin has also been proposed to exert anti-apoptotic effect on haemopoietic cells similar to bcl-2 that was also detected in such HCC samples. The activation of NANOG and particularly OCT4 in a number of cells in areas adjacent to erythrocytic clusters and co-expression with Glycophorin A in the same cell further confirms the HCC transdifferentiation into erythrocytic cell fate change before enucleation and cell death of such cells.

Cell signalling plays a key role not only in cancer growth and metastasis but also any cell fate changes that may take place under hypoxia, as the aberrant blood supply often creates a hypoxic microenvironment

within some areas of many tumours. The activation of multiple cell signalling pathways was observed in most HCC tumours in this study that could relate to multiple activities in such cells. VEGF and platelet-derived growth factor (PDGF) cell signalling was observed in most HCC tumours as VEGF is known to promote angiogenesis and both VEGF and PDGF cytokines are known to regulate the control of blood cell formation.<sup>24</sup> Angiogenesis in such regions, however, was not observed despite the detection of VEGF. Xue et al.<sup>25</sup> have also reported PDGF-BB to promote tumour growth, angiogenesis and extramedullary haemopoiesis at least in part through modulation of Epo activation. Hedgehog identified by Gli1/ptcl activation and BMP signalling identified by Smad158/BMPRI activation is also known to play multiple roles in tumour growth, stress erythropoiesis and erythroid differentiation.<sup>26,27</sup>

Despite the activation of multiple cell signalling pathways, Wnt signalling was one of the major cell signalling pathways activated in HCC tissues. A number of HCCs activating canonical Wnt signalling also showed the activation of Sulf1/Sulf2 enzymes that are usually undetectable in normal liver.<sup>18</sup> Canonical Wnt signalling was activated in most canine HCC tissues showing erythropoiesis in the present study as detected by the expression of Wnt2 ligand and nuclear  $\beta$ -catenin translocation. In addition to its role in tumour growth, canonical Wnt signalling thus could drive hepatoblast to erythroblast transdifferentiation in such HCCs. Both Sulf1 and Sulf2 have been shown to promote Wnt signalling<sup>28–30</sup> that further supports the transdifferentiation of hepatoblast to erythroblasts by Wnt signalling. In conclusion, immunocytochemical and mRNA analysis by RT PCR in this study demonstrates the transdifferentiation of hepatocytic cells into erythrocytes without the generation of blood vessels for circulation. It also shows that dysregulated cancer cell adaptation under stress does not benefit the tumour but imposes additional unsustainable metabolic demands to compensate for the loss of tumour cells in such regions. Further in vitro studies would determine if only specific cancer mutations or whether even some normal hepatocytes have the potential to transdifferentiate under hypoxia and the key signalling pathways that drive such changes in vivo.

#### Declaration of conflicting interests

The author(s) declared no potential conflicts of interest with respect to the research, authorship, and/or publication of this article.

#### Funding

The author(s) disclosed receipt of the following financial support for the research, authorship, and/or publication of this article: Abigail Hughes was supported by BBSRC research

studentship and the RVC funding was used to pay for the publication of this article.

#### ORCID iD

Gurtej K Dhoot  <https://orcid.org/0000-0002-1963-6522>

#### References

- Mittal S and El-Serag HB. Epidemiology of hepatocellular carcinoma: consider the population. *J Clin Gastroenterol* 2013; 47: S2–S6.
- Gill RM, Michael A, Westley L, et al. SULF1/SULF2 splice variants differentially regulate pancreatic tumour growth progression. *Exp Cell Res* 2014; 324(2): 157–171.
- Vander Heiden MG, Cantley LC and Thompson CB. Understanding the Warburg effect: the metabolic requirements of cell proliferation. *Science* 2009; 324(5930): 1029–1033.
- Warburg OS. On the origin of cancer cells. *Science* 1956; 123: 309–314.
- Kroemer G and Pouyssegur J. Tumor cell metabolism: cancer's Achilles' heel. *Cancer Cell* 2008; 13(6): 472–482.
- Garber K. Energy deregulation: licensing tumors to grow. *Science* 2006; 312(5777): 1158–1159.
- Gatenby RA and Gillies RJ. Why do cancers have high aerobic glycolysis? *Nat Rev Cancer* 2004; 4(11): 891–899.
- Jones RG and Thompson CB. Tumor suppressors and cell metabolism: a recipe for cancer growth. *Genes Dev* 2009; 23(5): 537–548.
- Lizama CO, Hawkins JS, Schmitt CE, et al. Repression of arterial genes in hemogenic endothelium is sufficient for haematopoietic fate acquisition. *Nat Commun* 2015; 6(7739): 7739.
- De Rosamel L and Blanc JF. Emerging tyrosine kinase inhibitors for the treatment of hepatocellular carcinoma. *Expert Opin Emerg Drugs* 2017; 22(2): 175–190.
- Hass HG, Vogel U, Scheurlen M, et al. Gene-expression analysis identifies specific patterns of dysregulated molecular pathways and genetic subgroups of human hepatocellular carcinoma. *Anticancer Res* 2016; 36(10): 5087–5095.
- Lenox LE, Shi L, Hegde S, et al. Extramedullary erythropoiesis in the adult liver requires BMP-4/Smad5-dependent signaling. *Exp Hematol* 2009; 37(5): 549–558.
- Ma F, Ebihara Y, Umeda K, et al. Generation of functional erythrocytes from human embryonic stem cell-derived definitive hematopoiesis. *Proc Natl Acad Sci U S A* 2008; 105(35): 13087–13092.
- Gill RM, Mehra V, Milford E, et al. Short SULF1/SULF2 splice variants predominate in mammary tumours with a potential to facilitate receptor tyrosine kinase-mediated cell signalling. *Histochem Cell Biol* 2016; 146(4): 431–444.
- Zanetta L, Marcus SG, Vasile J, et al. Expression of von Willebrand factor, an endothelial cell marker, is up-regulated by angiogenesis factors: a potential method for objective assessment of tumor angiogenesis. *Int J Cancer* 2000; 85(2): 281–288.
- Zaman G, Staines KA, Farquharson C, et al. Expression of Sulf1 and Sulf2 in cartilage, bone and endochondral fracture healing. *Histochem Cell Biol* 2016; 145(1): 67–79.

17. Gill RB, Day A, Barstow A, et al. Sulf2 gene is alternatively spliced in mammalian developing and tumour tissues with functional implications. *Biochem Biophys Res Commun* 2011; 414(3): 468–473.
18. Gill RB, Day A, Barstow A, et al. Mammalian Sulf1 RNA alternative splicing and its significance to tumour growth regulation. *Tumour Biol* 2012; 33(5): 1669–1680.
19. Oka M, Moriyama T, Asally M, et al. Differential role for transcription factor Oct4 nucleocytoplasmic dynamics in somatic cell reprogramming and self-renewal of embryonic stem cells. *J Biol Chem* 2013; 288(21): 15085–15097.
20. Qi C, Zhang J, Chen X, et al. Hypoxia stimulates neural stem cell proliferation by increasing HIF1alpha expression and activating Wnt/beta-catenin signaling. *Cell Mol Biol* 2017; 63(7): 12–19.
21. Acs G, Chen M, Xu X, et al. Autocrine erythropoietin signaling inhibits hypoxia-induced apoptosis in human breast carcinoma cells. *Cancer Lett* 2004; 214(2): 243–251.
22. Hudson JB, Murad FM, Kunkel JE, et al. Endoscopic ultrasound guided fine-needle aspiration of a splenic hemangioma with extramedullary hematopoiesis. *Diagn Cytopathol* 2013; 41(12): 1086–1090.
23. Liang J, Wan M, Zhang Y, et al. Nanog and Oct4 associate with unique transcriptional repression complexes in embryonic stem cells. *Nat Cell Biol* 2008; 10(6): 731–739.
24. Duhrsen U, Martinez T, Vohwinkel G, et al. Effects of vascular endothelial and platelet-derived growth factor receptor inhibitors on long-term cultures from normal human bone marrow. *Growth Factors* 2001; 19(1): 1–17.
25. Xue Y, Lim S, Yang Y, et al. PDGF-BB modulates hematopoiesis and tumor angiogenesis by inducing erythropoietin production in stromal cells. *Nat Med* 2011; 18(1): 100–110.
26. Maegdefrau U, Amann T, Winklmeier A, et al. Bone morphogenetic protein 4 is induced in hepatocellular carcinoma by hypoxia and promotes tumour progression. *J Pathol* 2009; 218(4): 520–529.
27. Roy A, Haldar S, Basak NP, et al. Molecular cross talk between Notch1, Shh and Akt pathways during erythroid differentiation of K562 and HEL cell lines. *Exp Cell Res* 2014; 320(1): 69–78.
28. Dhoot GK, Gustafsson MK, Ai X, et al. Regulation of Wnt signaling and embryo patterning by an extracellular sulfatase. *Science* 2001; 293(5535): 1663–1666.
29. Ai X, Do AT, Lozynska O, et al. QSulf1 remodels the 6-O sulfation states of cell surface heparan sulfate proteoglycans to promote Wnt signaling. *J Cell Biol* 2003; 162(2): 341–351.
30. Nawroth R, Van Zante A, Cervantes S, et al. Extracellular sulfatases, elements of the Wnt signaling pathway, positively regulate growth and tumorigenicity of human pancreatic cancer cells. *PLoS ONE* 2007; 2(4): e392.